



ELSEVIER

Tectonophysics 349 (2002) 185–201

TECTONOPHYSICS

www.elsevier.com/locate/tecto

Lateral thinking: 2-D interpretation of thermochronology in convergent orogenic settings

Geoffrey E. Batt^{a,*},¹ Mark T. Brandon^b

^aDepartment of Geology, Royal Holloway, University of London, Egham, Surrey TW20 0EX, UK

^bDepartment of Geology and Geophysics, Yale University, P.O. Box 208109, New Haven, CT 06520-8109, USA

Received 9 May 2000; accepted 16 October 2001

Abstract

Lateral motion of material relative to the regional thermal and kinematic frameworks is important in the interpretation of thermochronology in convergent orogens. Although cooling ages in denuded settings are commonly linked to exhumation, such data are not related to instantaneous behavior but rather to an integration of the exhumation rates experienced between the thermochronological ‘closure’ at depth and subsequent exposure at the surface. The short spatial wavelength variation of thermal structure and denudation rate typical of orogenic regions thus renders thermochronometers sensitive to lateral motion during exhumation. The significance of this lateral motion varies in proportion with closure temperature, which controls the depth at which isotopic closure occurs, and hence, the range of time and length scales over which such data integrate sample histories. Different chronometers thus vary in the fundamental aspects of the orogenic character to which they are sensitive. Isotopic systems with high closure temperature are more sensitive to exhumation paths and the variation in denudation and thermal structure across a region, while those of lower closure temperature constrain shorter-term behaviour and more local conditions. Discounting lateral motion through an orogenic region and interpreting cooling ages purely in terms of vertical exhumation can produce ambiguous results because variation in the cooling rate can result from either change in kinematics over time or the translation of samples through spatially varying conditions. Resolving this ambiguity requires explicit consideration of the physical and thermal framework experienced by samples during their exhumation. This can be best achieved through numerical simulations coupling kinematic deformation to thermal evolution. Such an approach allows the thermochronological implications of different kinematic scenarios to be tested, and thus provides an important means of assessing the contribution of lateral motion to orogenic evolution. © 2002 Elsevier Science B.V. All rights reserved.

Keywords: Lateral motion; Thermochronology; Orogenic regions

1. Introduction

Thermal histories of rocks provide important constraint on geological models, particularly in regions of

orogenic activity. Such regions are typically characterized by rapid uplift and denudation, which prevents many stratigraphic and structural records of tectonic evolution being preserved over the long-term at the surface. The thermochronological ages of metamorphic and plutonic rocks exposed by erosion and tectonic denudation, in contrast, are directly related to cooling caused by the exhumation experienced (e.g. Hurley et al., 1962; Clark and Jäger, 1969; Kamp et al., 1989;

* Corresponding author. Fax: +44-1784-471-780.

E-mail address: g.batt@gl.rhul.ac.uk (G.E. Batt).

¹ Formerly at the Department of Geology and Geophysics, Yale University, P.O. Box 208109, New Haven, CT 06520-8109, USA.

Tippett and Kamp, 1993). Each chronometer is sensitive to a particular range of temperatures, or in more elementary interpretations, to a particular ‘effective closure temperature’ (Dodson, 1973). These isotopic ages provide an important window into the evolution of denuded regions and workers have long utilized thermochronology to gain understanding of orogenic development and dynamics (e.g. Clark and Jäger, 1969; England and Richardson, 1977; Zeitler et al., 1982; Copeland et al., 1987; Ruppel et al., 1988; Ruppel and Hodges, 1994; Harrison et al., 1995, 1996).

The relative uplift and exhumation at the core of this approach are fundamentally driven by lateral motion between crustal and, at a larger scale, lithospheric blocks. This is of particular significance in orogenic regions, where crustal structure and kinematics (e.g. Beaumont et al., 1992, 1996; Koons, 1994), thermal structure (e.g. Koons, 1987; Lewis et al., 1988; Hyndman and Wang, 1993; Batt and Braun, 1997) and regional exhumation rates (e.g. Wellman, 1979; Zeitler et al., 1982; Brandon et al., 1998) can all have strong lateral gradients. Material traversing this variable framework is subject to an accompanying range of conditions during its residence within the deforming region. This spatial integration of conditions and the tectonic juxtaposition of samples with widely varying kinematic history have been shown to be an important consideration in understanding the structural and metamorphic evolution of orogenic regions (e.g. Stüwe et al., 1994; Jamieson et al., 1996; Harrison et al., 1998).

This work examines the implications of integrating particle history in more than one dimension to the interpretation of thermochronology in orogenic regions. We begin by illustrating how the effects of 2-D motion relative to an orogenic framework are expressed on the varying time and length scales constrained by different thermochronometers and outlining how numerical modeling techniques can be used to address such effects. We then present case studies drawing on recent reinterpretations of thermochronological data from the Olympic Mountains of Washington State and the Southern Alps of New Zealand. These examples illustrate the potential ambiguity of a one-dimensional interpretation of isotopic chronology in regional dynamical studies and show how consideration of the lateral motion of material can lead to improved understanding.

2. Tectonic interpretation of thermochronology

The products of radioactive decay within a crystal are generally highly mobile and are only quantitatively retained if a sample is cold enough that they lack the energy to diffuse through the crystal lattice (Dodson, 1973). The thermal dependence of this diffusive loss is commonly simplified through the concept of closure temperature, representing the temperature of transition from effectively open system loss of a radiogenic daughter product to its complete retention on geological time scales (Dodson, 1973). Fission tracks are similarly unstable at elevated temperatures, with the radiogenic lattice damage that forms the basis of etchable ‘tracks’ in crystals progressively healing over time, shortening and eventually eliminating the tracks. An analogous simplification is again commonly made of reducing this complex annealing behavior to a concept of ‘closure’ of fission track dating systems as rocks cool through the partial retention zone (PRZ) relevant to fission tracks in a given mineral (e.g. Naeser, 1979; Gleadow and Duddy, 1981; Naeser et al., 1989).

These thermochronological relationships are often exploited to provide constraint on regional geological history, based on an assumption that an apparent age reflects the time taken for sample exhumation after cooling through the relevant closure temperature (e.g. England and Richardson, 1977; Ruppel et al., 1988; Ruppel and Hodges, 1994; Batt et al., 2000). It should be noted that exhumation is specific to the reference frame of a given sample and is thus not directly interchangeable (other than in a simplified 1-D case) with spatial parameters such as erosion or tectonic unroofing. This terminology is reviewed at length by Ring et al. (1999) and we adopt their suggested usage here. Exhumation refers to the unroofing history of an actual rock, defined as the vertical distance traversed relative to the Earth’s surface. Denudation, taken in the broad generic sense of Ring et al. (1999), relates to the removal of material at a particular point at or under the Earth’s surface by tectonic processes and/or erosion and is more correctly viewed as a measure of material flux.

Thermochronological studies of regional tectonic development typically begin by assuming or calculating a specific geothermal structure, based on the rates of material advection and the thermal conductivity of

the rocks concerned (Mancktelow and Grasemann, 1997). Under steady kinematic conditions, thermal structure rapidly attains a corresponding stable form (e.g. Koons, 1987; Stüwe et al., 1994; Mancktelow and Grasemann, 1997), and hence, forms an Eulerian framework against which we can evaluate the relative motion of material. If this local geotherm is known (or can be reasonably well-estimated), cooling can be related to material motion relative to that thermal structure, providing insight into regional kinematics and tectonic evolution. Denudation rates, for example, are often calculated using either the difference in measured age between two chronometers with different closure temperatures for a single sample or the locality (the mineral pairs method of Wagner et al., 1977) or by the altitude and age differences between several samples of a single chronometer (most commonly fission tracks in apatite) across an area (the altitude dependence method) (e.g. Wagner and Reimer, 1972; Wagner et al., 1977; Fitzgerald and Gleadow, 1988). Variation in cooling is also viewed as indicative of tectonic events. Rapid increase or decrease in the cooling rate, for example, is often taken to represent the initiation or cessation of orogenic activity, respectively (e.g. Zeitler et al., 1982; Fitzgerald and Gleadow, 1988; Tippett and Kamp, 1993).

In the absence of strong dynamic forcing (e.g. Mancktelow and Grasemann, 1997) or the transient effects of magmatic intrusion, temperature increases with depth in the crust, with isotherms approximately parallel to topography near the surface, and becoming progressively more subdued with depth (e.g. Stüwe et al., 1994; Mancktelow and Grasemann, 1997). Exhumation of material through the thermally stratified crust is thus generally perceived as more important than lateral motion (which is predominantly parallel to the regional isotherms) in the cooling of geological samples. Such lateral motion is ignored accordingly in thermo-tectonic studies, with cooling typically equated directly to vertical exhumation (e.g. Tippett and Kamp, 1993; Mancktelow and Grasemann, 1997; Brandon et al., 1998).

Such a one-dimensional simplification becomes inadequate when the integrated transport and cooling histories of material in orogenic environments are considered. Both thermal structure (e.g. Koons, 1987; Lewis et al., 1988; Hyndman and Wang,

1993; Stüwe et al., 1994; Allis and Shi, 1995) and rates of uplift and exhumation (e.g. Wellman, 1979; Zeitler et al., 1982; Tippett and Kamp, 1993; Brandon et al., 1998) can vary dramatically across orogenic regions. Because isotopic ages effectively integrate the exhumation rates experienced between thermally controlled closure at depth and the subsequent exposure of a sample (Fig. 1), lateral motion of material relative to the orogenic framework (the geographical distribution of deformation and denudation and the steady state thermal structure of the region) exerts a considerable influence on the isotopic ages observed in tectonically active regions. Even though this lateral motion produces relatively little intrinsic cooling, such movement of material will affect the range of kinematic conditions experienced, the overall material path of a sample, and the thermal consequences of that path.

The potential thermochronological consequences of such motion relative to the orogenic framework are illustrated in Fig. 1. Material is assumed to be traversing a convergent orogen where denudation rates vary laterally across the region. For simplicity, thermal structure is shown as uniform, with a linear geothermal gradient. The illustrated sample progressively cools through the closure temperatures of three arbitrary ‘thermochronometers’ during its exhumation, experiencing thermochronological closure at points A, B, and C, respectively, with A', B', and C' marking the corresponding point at the surface directly above each of these sites. Upon its eventual exposure at the surface, the apparent ages of the sample for each of these three chronometers reflect the average exhumation rate experienced between the relevant point of closure (A, B, or C) and exposure of the sample at point D. Due to the lateral variation in denudation rate, the exhumation rate experienced varies through time as the sample traverses the deforming region. As a result, none of the chronometers indicated will accurately reflect the denudation rate at point D.

The importance of this averaging of conditions increases in proportion with closure temperature, due to the corresponding increase in the time and length scales over which conditions are integrated. For any given exhumation path, the higher the closure temperature concerned, the deeper a chronometer undergoes closure, the longer a sample takes to be

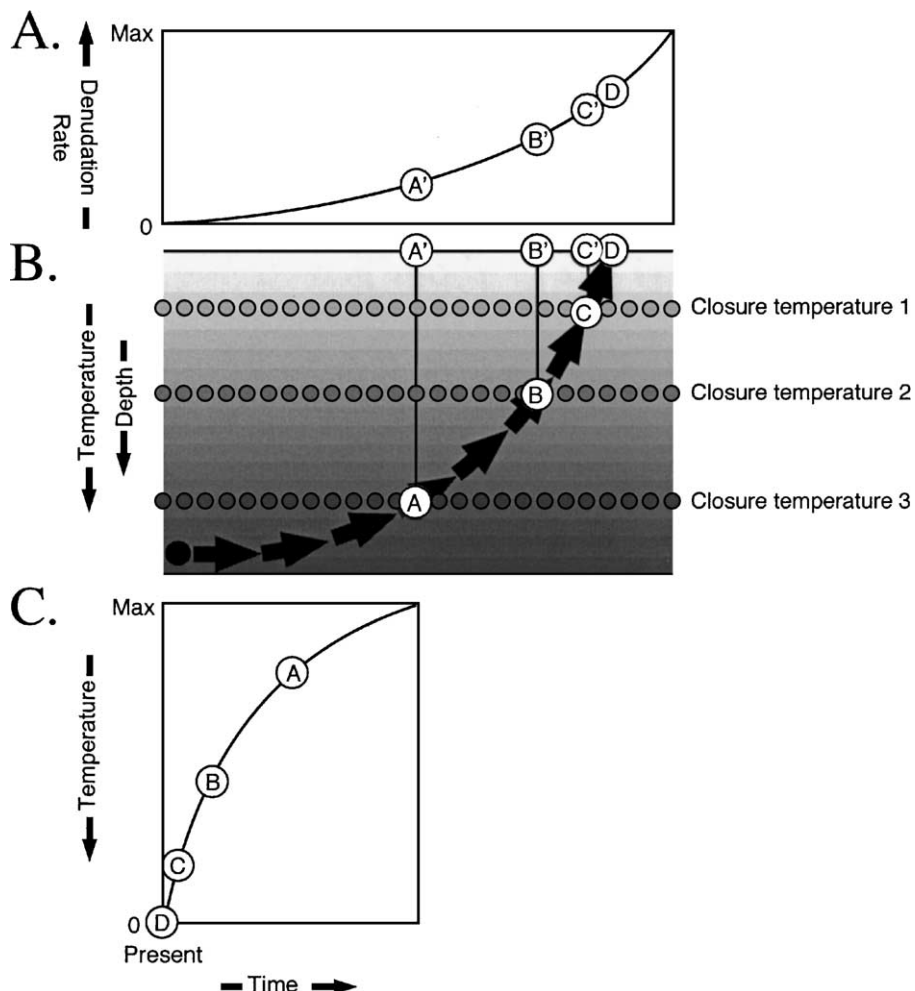


Fig. 1. Thermochronological significance of the material convergence relative to the denudational and thermal framework of a deforming region. Note that although figurative, the processes and effects illustrated are derived from published (Batt and Braun, 1997, 1999; Batt et al., 2001) and unpublished numerical modeling works of the authors. (A) Assumed variation in erosion rate across the area of interest, (B) regional thermal structure and the material path taken by a selected sample during its passage through the deforming region. Arbitrary closure temperatures are shown for three ‘thermochronometers’, as discussed in the text. (C) Variation in the temperature experienced over time by the particle illustrated in panel B. Note the progressive acceleration in the cooling rate. This is caused by spatial rather than temporal variation in the exhumation rate (panel A), and thus, illustrates the caution required in attaching the dynamic significance to such features.

exhumed following closure (i.e. the greater its age upon exposure at the surface), and hence, the greater the potential thermochronological consequences of lateral variation in orogenic character (Fig. 1). Closure of different thermochronometers at differing temperatures thus results in sensitivity to a corresponding range of time and length scales. The higher the closure temperature of a chronometer, the more sensitive its ages will be to the variations in thermal structure and

denudation rate across an orogen and to the specific exhumation path experienced. Conversely, the lower the closure temperature, the more sensitive a chronometer will be to short-term behavior and local conditions (Fig. 1).

Far from being an exceptional occurrence, such lateral motion dominates the overall kinematics experienced in many orogenic regions, with samples experiencing tens or even hundreds of kilometers of

lateral motion during progressive uplift and exhumation from the mid crustal depths (e.g. Beck, 1991; Jamieson et al., 1996; Walcott, 1998; Brandon and Vance, 1992; Brandon et al., 1998), and hence integrating orogenic conditions over potentially great distances (Fig. 1). As a guide to the potential significance of such lateral motion for a given region, consider the spatial variability in denudation rate:

$$\lambda_{\Delta\varepsilon} = \left(\frac{\varepsilon_{\max} - \varepsilon_{\min}}{\varepsilon_{\max}} \right) \div \lambda_{\Delta\varepsilon} \quad (1)$$

and the horizontal length scale of the sample travel between the closure at depth and exhumation at the surface (Fig. 1):

$$\lambda_x = v_h t_s \quad (2)$$

where ε_{\max} and ε_{\min} are the maximum and minimum denudation rates across the region, $\lambda_{\Delta\varepsilon}$ is the length scale over which this variation occurs, v_h is the rate of horizontal motion across the region, and t_s is the sample age. Multiplied together, these gave a dimensionless number:

$$\eta = \lambda_x f_{\Delta\varepsilon} \quad (3)$$

indicating the relative variation in exhumation rate which a sample may have experienced between thermochronological closure and its exposure at the surface. If either the variability in denudation rate ($\varepsilon_{\max} - \varepsilon_{\min}$) or the horizontal velocity v_h are small, η tends towards 0, and the thermochronological consequences of lateral motion can be discounted. Conversely, high values of η (approaching or in regions with particularly short wavelength variation in denudation rate, potentially exceeding 1) indicate that a sample is likely to experience a wide range of exhumation rates during its uplift and exhumation, with a corresponding influence on the age observed.

Despite this potential significance, the inability of lateral motion to produce a significant and predictable cooling effect in its own right renders the long-term horizontal rates of transport across orogenic regions difficult to constrain. This issue can be addressed through numerical simulations that incorporate the two- and three-dimensional kinematics of orogenic deformation and denudation, and thus allow the thermochronological record to be interpreted in the context of the overall motion experienced. Geological and structural controls, together with the requirements for material conservation, enable a reasonable approx-

imation to be made of the mode of deformation of many orogenic regions. Numerical models based on such kinematic frameworks can then be used to solve for the evolving thermal structure of the orogen (e.g. Koons, 1987; Beaumont et al., 1996; Batt and Braun, 1997). The physical and thermal coupling of these models enables the tracking of selected material points through the model domain and the assessment of how a given exhumation path interacts with the evolving thermal structure, enabling individual particle thermal histories (and their implications for different thermochronometers) to be calculated. The complex multivariate models needed to incorporate the dynamic interplay of heat flow, kinematics, and sample mineralogy that go into producing a thermochronological age (Fig. 1) cannot usually provide a unique interpretation for specific age data (e.g. Quidelleur et al., 1997). Rather, as illustrated in the following case studies, such models are used to provide insight into how various aspects of orogenic deformation are ultimately integrated in the thermochronological record, and thus help to choose between the competing hypotheses and guide interpretation of the physical causes behind regional patterns observed in thermochronological data (e.g. Shi et al., 1996; Beaumont et al., 1996; Batt and Braun, 1999; Batt et al., 2001).

3. Case study 1: tectonic character of the Olympic Mountains

The Olympic Mountains (Fig. 2) are the topographically highest and most deeply exhumed segment of the Cascadia forearc high. The Olympics were the earliest part of the forearc to become emergent at ca. 12 Ma (Brandon and Calderwood, 1990) and the mountainous topography of the range has been sustained since this time by continued accretion of material from the subducting Juan de Fuca Plate (Fig. 2) and within-wedge deformation (e.g. Brandon and Calderwood, 1990; Brandon et al., 1998). The Cascadia accretionary wedge (Fig. 2) is composed dominantly of sedimentary material built up by this progressive accretion (Clowes et al., 1987; Brandon and Calderwood, 1990). This sedimentary wedge underlies most of the offshore continental margin, reaching a thickness of 30 km but is only subaerially

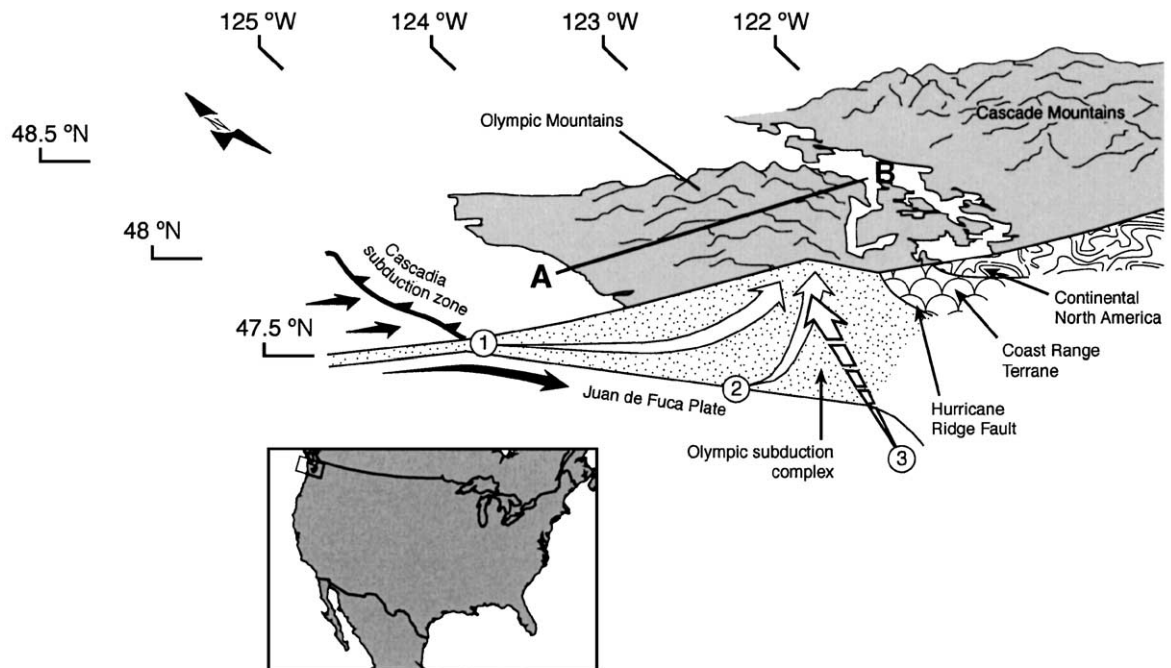


Fig. 2. Key geographical features of the Cascadia margin of North America, incorporating a figurative cross-section illustrating the structural and tectonic nature of the Olympic section of the Cascadia wedge, after Brandon et al. (1998). Line A–B indicates the approximate position of the thermochronological transect shown in Fig. 3. The white arrows illustrate the material flux paths suggested by the competing hypotheses of the Olympic orogen kinematics: (1) frontal accretion of the incoming sedimentary section of the Juan de Fuca plate at the toe of the Cascadia wedge (e.g. Davis and Hyndman, 1989), (2) underplating of subducted material at depth beneath the orogen (e.g. Clowes et al., 1987; Brandon and Calderwood, 1990), and (3) margin-parallel transport (e.g. Beck, 1991; McCaffrey and Goldfinger, 1995; McCaffrey, 1996; McCrory, 1996; Wang, 1996). Note that arrows 1 and 2 are in, and arrow 3 is perpendicular to, the plane of the illustrated section.

exposed in the Olympic Mountains (Stewart, 1970; Rau, 1973; Tabor and Cady, 1978a,b).

In common with many accretionary complexes, there is a general paucity of age diagnostic fossils within the sandstones of the Cascadia accretionary wedge. Further, those fossils that are found are typically from unusual, possibly allochthonous rock units, such as isolated blocks of limestone, chert, or pillow basalt (Brandon and Vance, 1992). In the absence of reliable paleontological age control, thermochronological data have been the prime means of constraining the tectonic evolution of the Olympic orogen. Dating of detrital grains from sandstones of the accretionary wedge has been used to better define the timing of subduction, accretion, and metamorphism of rocks within the complex, and thus evaluate the progressive evolution of the region (e.g. Tabor, 1972;

Brandon and Vance, 1992; Brandon et al., 1998; Batt et al., 2001; Dick Stewart, unpublished data). This record is complemented by a growing data set of apatite (U–Th)/He ages (Batt et al., 2001; and unpublished data of the authors). Ages are generally youngest in the more deeply exhumed interior of the orogen and increased markedly towards the eastern and western boundaries of the Olympic Peninsula (Fig. 3). Notably, the age minima of the zircon and apatite fission track chronometers are offset from one another by some 20 km (Fig. 3).

Competing hypotheses as to the primary mechanism driving the ongoing uplift of the Olympic Mountains center on (1) frontal accretion of the incoming Juan de Fuca plate sedimentary section at the toe of the Cascadia accretionary wedge (e.g. Davis and Hyndman, 1989), (2) underplating of subducted

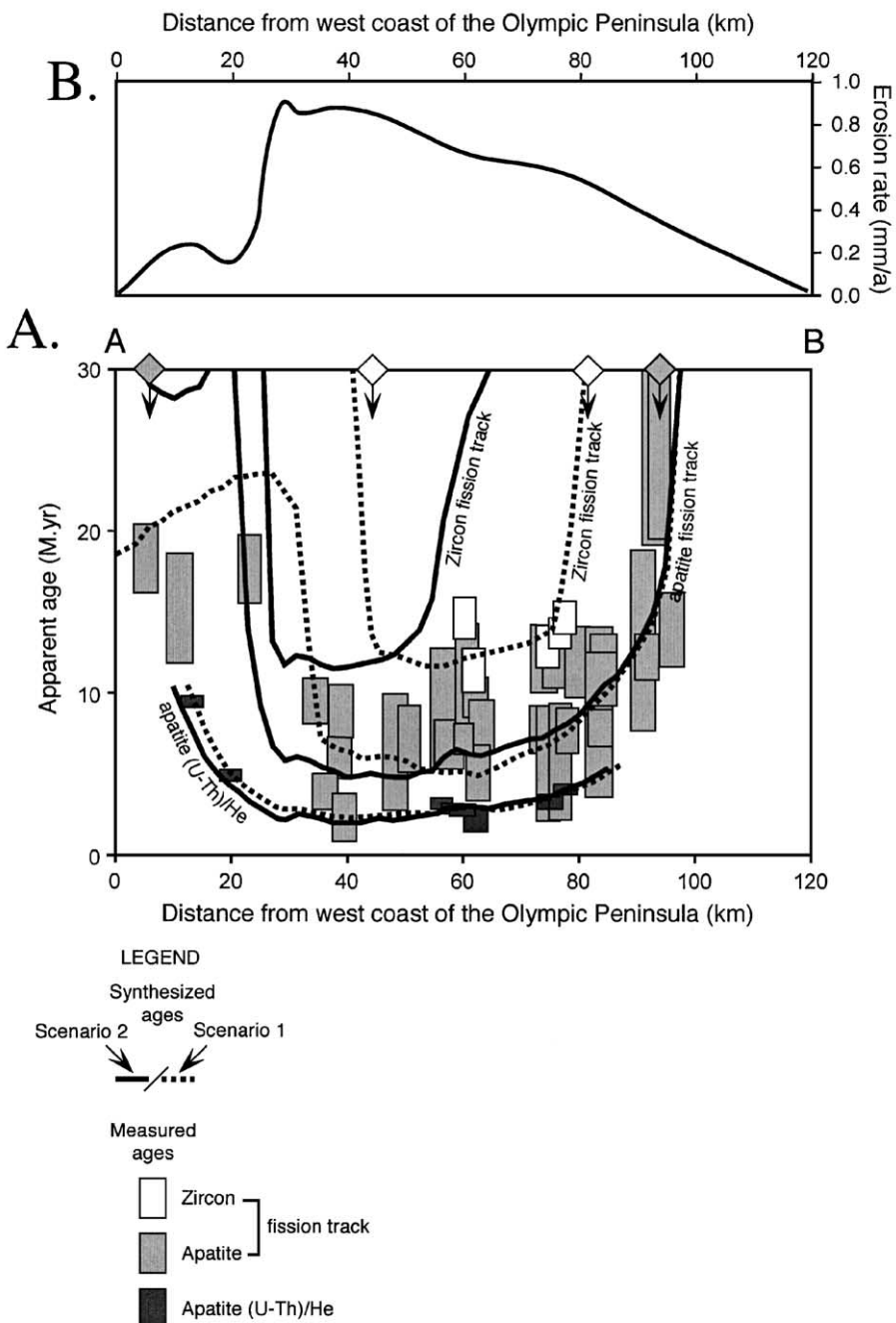


Fig. 3. (A) Thermochronological age variation across the Olympic orogen plotted as apparent age vs. distance along section A–B in Fig. 2. Zircon fission track ages came from Brandon and Vance (1992) and Garver and Brandon (1994), apatite fission track ages from Brandon et al. (1998) and Roden-Tice (unpublished data), and (U–Th)/He ages are taken from Batt et al. (2001) and unpublished data of the authors. The shaded symbols straddling the upper margin of the chart indicate the transition to inherited or ‘unreset’ ages off the scale of this figure for the respective fission track data sets. The curves plotted represent the results of 2-D dynamical models discussed in detail by Batt et al. (2001), comparing the relative thermochronological implications of kinematic scenarios 1 and 2 (Fig. 2), as discussed in the text. (B) Recent erosion rates across the Olympic Peninsula, calculated from the apatite fission track ages and deformed and offset river terraces, after Pazzaglia and Brandon (in review).

material at depth beneath the orogen (e.g. Clowes et al., 1987; Brandon and Calderwood, 1990), and (3) margin-parallel transport (e.g. Beck, 1991; McCaffrey and Goldfinger, 1995; McCaffrey, 1996; McCrory, 1996; Wang, 1996) (Fig. 2).

Previous 1-D interpretations of thermochronological data from the Olympics (Brandon et al., 1998) are unable to test the relative merits of these kinematic scenarios (Fig. 2), as the differences between the three lie primarily in the relative importance and orientation of lateral material motion through the deforming orogen. In scenario 1, the sedimentary cover of the Juan de Fuca plate is incorporated into the Olympic subduction complex at the toe of the Cascadia accretionary wedge. Exposure in the forearc high thus requires progressive advection of this accreted material through the wedge, with resultant sensitivity to variation in exhumation rates and thermal structure across the Olympic Peninsula (Fig. 1). In scenario 2, sedimentary material is carried beneath the Cascadia wedge by the subducting Juan de Fuca plate and incorporated into the accretionary wedge by underplating at depth beneath the eroding forearc high. Subsequent exhumation of this material would be very steep, with little lateral motion of material relative to the physical and thermal framework of the wedge post-dating thermochronological closure. In scenario 3, lateral motion of material relative to the orogenic framework is dominantly parallel to the plate margin, with resulting sensitivity to the north–south variation in character across the orogen, as opposed to east–west (Fig. 2).

Pazzaglia and Brandon (2001) refuted major margin-parallel deformation by using deformed erosional benchmarks to estimate the long-term permanent strain rates across the Olympic Peninsula. Offset of fluvial terraces on the western side of the Olympics indicates strain across the orogen (approximately parallel to line A–B in Fig. 2) at 3×10^{-2} $\mu\text{strain}/\text{year}$. A deformed 125 ka unconformity (the Sangamin high stand) that runs along the west coast of the Olympic Peninsula for 80 km (McCrory, 1996) indicates a long-term margin-parallel strain rate (north–south) of only 8×10^{-7} $\mu\text{strain}/\text{year}$, five orders of magnitude slower than the margin-perpendicular rate. This contrast essentially rules out scenario 3 as a major factor in the evolution of the Olympic Mountains as it prevents the development of a viable kine-

matic model dominated by the margin-parallel motion of the material.

Building on this conclusion, Batt et al. (2001) modeled the dynamic and thermal evolution of the Olympic subduction complex in two-dimensions parallel to Juan de Fuca plate convergence. Incorporating available constraints on heat flow and erosion rates, they test the relative validity of scenarios 1 and 2 by assessing how the differing kinematic conditions should affect thermochronological ages at the surface of the orogen.

Eq. (3) allows us to quantify the potential significance of lateral motion to the interpretation of thermochronology for these scenarios. Denudation rates vary from 0 at the western margin of the Olympic Peninsula to a peak of ca. 1 mm/year in the region of Mt. Olympus 30 km to the east (Brandon et al., 1998; Pazzaglia and Brandon, 2001) (Fig. 3). The dynamic models of Batt et al. (2001) predicted an eastward horizontal material velocity at the west coast of the Olympic Peninsula (relative to the steady state orogenic framework) of ca. 4 mm/year for scenario 1 (frontal accretion) and 0 for scenario 2 (underplating). Minimum ages observed across the orogen are approximately 2 Ma for the apatite (U–Th)/He chronometer, 5 Ma for fission tracks in apatite, and 13 Ma for fission tracks in zircon (Fig. 3). For scenario 1, these values yield η equal to 0.27 for apatite (U–Th)/He ages (indicating a potential maximum 27% variation in the exhumation rate between the thermochronological closure and exposure at the surface), 0.67 for apatite fission track ages, and 1.73 for zircon fission track ages. The high value for zircon reflects the fact that the predicted lateral travel of samples for this chronometer subsequent to closure exceeds the 30-km length scale of variation in denudation. For scenario 2, the negligible lateral transport rate translates into η equal to 0 for any chronometer.

Under scenario 1, the variation in η is expressed as a relative disparity between the strongly asymmetric denudation rate variation across the Olympics and the ages observed (Fig. 3). For the Cascadia wedge regime, dominated as it is by eastward convergence and accretion (Fig. 2), the minimum modeled ages are offset to the east of the highest erosion rates. This offset is progressively greater for apatite (U–Th/He), apatite fission track, and zircon fission track ages, in

accordance with the relative values of η calculated (Fig. 3). As noted above, the observed distribution of ages across the Olympic Peninsula displays just such a relative offset between the spatial variation, particularly the age minima, of different chronometers (Fig. 3).

In the underplating-dominated setting of scenario 2, no such offset develops. Instead, relative geographical variation in denudation rate is reflected directly in model ages (as predicted by the η value of 0), producing a pseudo-one-dimensional orogenic character with the age of all chronometers varying in phase with one another across the region (Fig. 3). The 2-D modeling approach of Batt et al. (2001) thus apparently resolves the ambiguity of these competing physical models, favoring the frontal accretion of sediment at the toe of the Cascadia accretionary wedge (scenario 1) as the simplest consistent explanation for the thermochronological variation observed across the Olympics.

In Fig. 4, we illustrate the specific significance of lateral motion in this preferred scenario for individual samples. Here, we explicitly compare the apatite fission track ages modeled by Batt et al. (2001) for an Olympic orogen controlled by frontal accretion (Fig. 1) with the 1-D analysis previously afforded to thermochronology in the Olympics by Brandon et al. (1998). Dynamic perturbation of the initial thermal profile in the 1-D analysis (e.g. Clark and Jäger, 1969; Oxburgh and Turcotte, 1974; England and Thompson, 1984) is approximated using a steady state solution for a 1-D layer of thickness L . The upper and lower boundaries of the layer are held at constant temperatures T_s and $T_s + g_0/L$, respectively, where T_s is the temperature at the surface, and g_0 is the geothermal gradient. The accretion rate at the base of the layer is equal to the denudation rate at the top of the layer, resulting in a constant material velocity within the layer. The steady state temperature profile is given by (Eq. (8) in Stüwe et al., 1994):

$$T(z, \dot{e}) = T_s + g_0 L \frac{1 - e^{-\dot{e}z/\kappa}}{1 - e^{-\dot{e}L/\kappa}} \quad (4)$$

where z is the depth of the point in question and κ is the thermal diffusivity of the medium. For the sediment-rich Cascadia accretionary wedge, $\kappa \approx 20 \text{ km}^2/\text{Ma}$ (Brandon and Vance, 1992). Brandon et al. (1998)

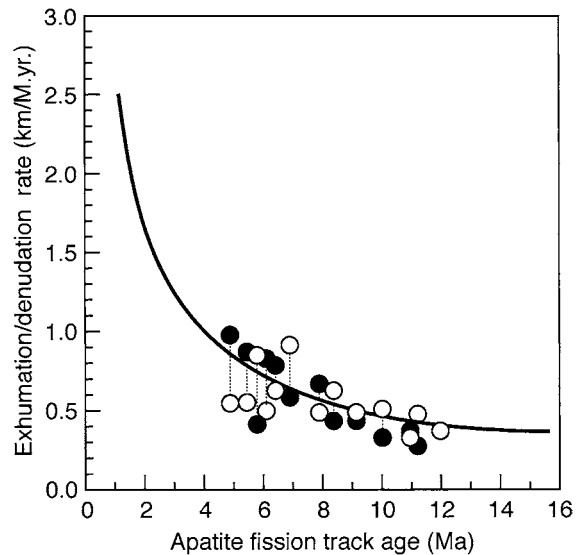


Fig. 4. Relationship of modeled fluorapatite fission track ages at the surface of the Olympics to exhumation rate. Solid line marks the 1-D relationship, calculated after Brandon et al. (1998), for a 20-km-thick crustal layer, assuming the thermal diffusivity of $20 \text{ km}^2/\text{Ma}$ and a thermal structure at equilibrium, as discussed in the text. Paired circular symbols represent the corresponding relationship for individual samples analyzed in a 2-D model of the Cascadia accretionary wedge-forearc system (Batt et al., 2001) (Fig. 3). Open circles mark the denudation rate at the site of a sample's exposure at the surface, with filled circles marking the exhumation rate experienced at the modeled time of closure.

settled on a thickness, L , of 20 km, which approximates the average thickness of the rear part of the accretionary wedge since Middle Miocene time (Brandon et al., 1998).

The effective closure temperature of a sample T_c can be calculated as a function of its cooling rate. An approximate relationship for this effect is given by Eq. (11) in Dodson (1979):

$$\dot{T} = \frac{-RT_c^2}{E Be^{E/RT_c}} \quad (5)$$

where R is the gas constant, E is the activation energy of the system, and B is a proportionality constant. The constants in Eq. (5) can be derived from annealing data for Durango fluorapatite from Laslett et al. (1987). $E_{50\%} = 44.65 \text{ kcal/mol}$ and $B = 3.223 \times 10^{-26} \text{ Ma}$.

The actual cooling rate at closure is a function of the exhumation rate of the sample and the vertical gradient in the temperature profile at T_c :

$$\dot{T}(T_c) = \frac{dT}{dz} \frac{dz}{dt} = \frac{\dot{\varepsilon}^2}{\kappa} \left(\frac{g_0 L}{1 - e^{-\dot{\varepsilon}L/\kappa}} - T_c - T_s \right). \quad (6)$$

Eq. (4) is inverted to define z_c , the depth at which closure occurs:

$$z_c = -\frac{\kappa}{\dot{\varepsilon}} \ln \left(1 - \frac{T_c - T_s}{g_0 L} \left(1 - e^{-\dot{\varepsilon}L/\kappa} \right) \right). \quad (7)$$

A final equation relates z_c to the fission track age τ and the constant exhumation rate $\dot{\varepsilon}$:

$$z_c = \dot{\varepsilon}\tau. \quad (8)$$

Combining Eqs. (5, 6 and 7) with Eq. (8) gives two equations which Brandon et al. (1998) solved numerically for the two unknowns, $\dot{\varepsilon}$ and T_c , giving the relationship shown by the solid curve in Fig. 4.

Batt et al. (2001) applied an analogous process in two-dimensions to predict the ages in their numerical models (Fig. 3), solving for the dynamic effects of material motion and denudation on thermal structure, assessing the passage of individual samples through the thermal field, and deriving model ages from the resulting thermal history. In one conceptual difference of note between the two approaches, Batt et al. (2001) modeled the actual annealing of fission tracks in the samples. Given that the closure temperature calculation of Brandon et al. (1998) is derived as a numerical simplification of this behavior, however, the two approaches should yield comparable ages for a given thermal history, except for those samples exhumed from the specific narrow partial retention zone for the chronometer in question. Because of the lateral variation in $\dot{\varepsilon}$, local denudation rates at the sites where most samples in the 2-D model are eventually exposed differ significantly from the rates to which the local thermal structure was equilibrated at the point of closure (Fig. 4). As a result, no simple relationship can be drawn between the age of a sample and the local dynamics of the crust. As shown in Fig. 4, ignoring this effect and interpreting these apatite fission track ages under the assumption of 1-D behavior could result in errors in the estimated local denudation rate approaching the theoretical 67% level predicted in the η analysis above. This interpretational

error would be proportionately magnified for zircon fission track ages and other chronometers of higher closure temperature (Fig. 1).

4. Case study 2: the Southern Alps of New Zealand

Convergence between the Australian and Pacific plates through the South Island of New Zealand has given rise to the Southern Alps, a prominent linear mountain range running almost the length of the island (Fig. 5) (e.g. DeMets et al., 1990; Norris et al., 1990; Pearson et al., 1995). Uplift rates in the Southern Alps reach the order of 10 mm/year adjacent to the Alpine Fault (Wellman, 1979; Adams, 1980) but correspondingly rapid erosion (Tippett and Kamp, 1993) and removal of material into the Tasman Sea by the efficient network of rivers along the western front of the range effectively pin the range front at the Alpine Fault (Fig. 5). This erosion has prevented significant overthrusting by the Pacific Plate and orogenic growth, despite an estimated 90 ± 20 km of convergence (Walcott, 1998) over the past ca. 5 Ma (Sutherland, 1996; Batt et al., 1999, 2000; Chamberlain et al., 1999).

The rapid erosion of the Southern Alps leaves little physical record of the orogen's early development at the surface (for exceptions in the sedimentary record, see Cutten, 1979; Sutherland, 1994, 1996), and workers have long utilized geochronology to investigate the dynamic history of the orogen (e.g. Adams and Gabites, 1985; Tippett and Kamp, 1993; Shi et al., 1996; Batt et al., 1999, 2000). The most comprehensive studies to date are those of Peter Kamp and co-workers (e.g. Kamp et al., 1989; Tippett and Kamp, 1993, 1995; Kamp and Tippett, 1993; Kamp, 1997) examining the zircon and apatite fission track record of the orogen.

Kamp et al. (1989) and Tippett and Kamp (1993), in particular, demonstrated that both cooling ages and the thermally significant exhumed partial retention zones of fission tracks in apatite and zircon can be coherently mapped across the Southern Alps. These studies provide important constraint on the thermal structure and deformation history of the orogen and have formed the foundation of much of the subsequent thermo-tectonic work in the Southern Alps (e.g. Shi et al., 1996; Batt et al., 2000). In their physical interpretation of the data however, Kamp et al. (1989)

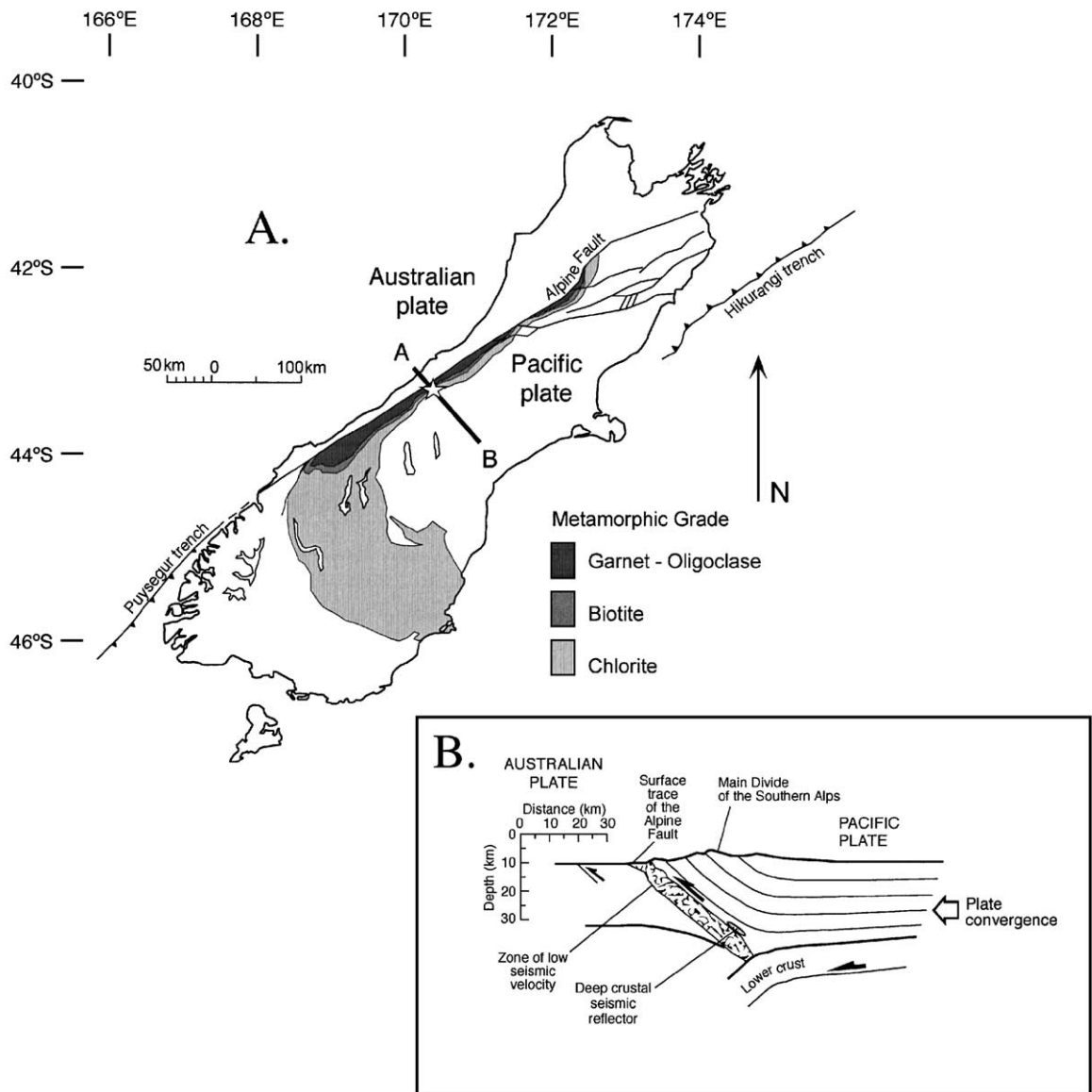


Fig. 5. (A) Major geological features of the Southern Alps and localities mentioned in the text, simplified from Grapes and Watanabe (1992). The star shown in the central region of the orogen indicates the approximate location of the samples discussed in relation to Fig. 6. Line A–B indicates the approximate location of the section shown in panel B. (B) Figurative section summarizing the geophysical constraint of the crustal structure beneath the Southern Alps. This illustrative section is a composite sketch, drawing on the results of Reyners and Cowan (1993), Smith et al. (1995), Stern (1995), and Davey et al. (1995).

and Tippett and Kamp (1993) effectively worked in a one-dimension, equating cooling purely to exhumation and interpreting any changes in cooling rate to reflect variation in local conditions through time.

As illustrated by Walcott (1998), this approach is ineffective when applied to the manifestly three-dimensional Southern Alps. Uplift of the Southern Alps is driven by comparably rapid convergence between the

Australian and Pacific Plates at ca. 12 mm/year (e.g. DeMets et al., 1990; Walcott, 1998). The spatial variation in denudation rate (from approximately 11 mm/year adjacent to the Alpine Fault to 1 mm/year 30

km to the east (Tippett and Kamp, 1993)) and thermal structure (Fig. 6) across the Southern Alps accordingly play a significant role in the cooling and exhumation experienced during residence in the orogen.

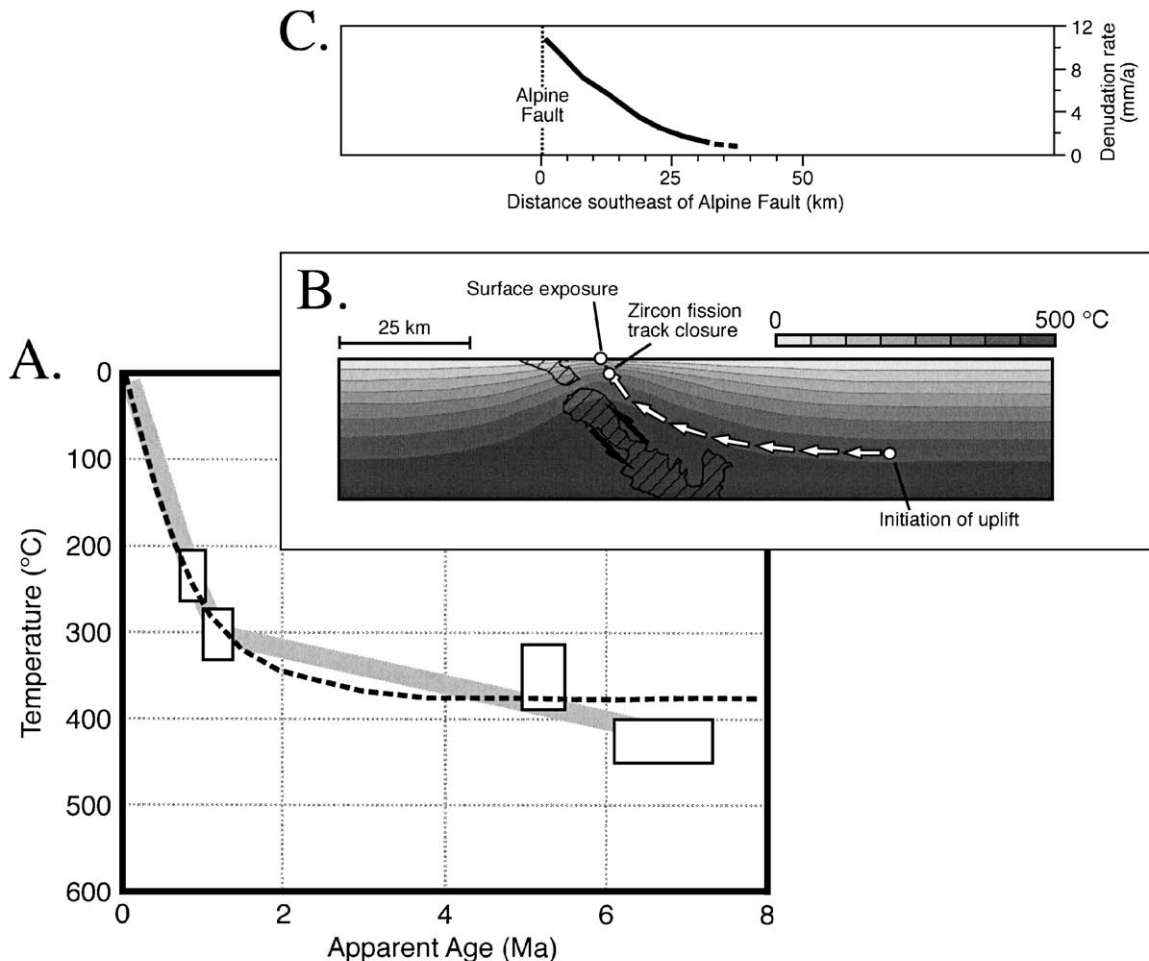


Fig. 6. Interpretation of cooling histories experienced in the Southern Alps. (A) Grey curve shows the cooling history experienced by rocks adjacent to the Alpine Fault in the central Southern Alps (Fig. 5), after Tippett and Kamp (1993). Constraints indicated by the white boxes correspond to, in order of increasing temperature, zircon fission track ages (Tippett and Kamp, 1993), biotite and muscovite K–Ar ages (Adams, 1981), and the inferred pre-uplift temperature of the region (Tippett and Kamp, 1993). The overlain black dotted curve indicates the cooling history of a particle passing through a 2-D simulation of the Southern Alps over 5 Ma, as indicated in panel B. (B) Numerical model results illustrating the exhumation history of a particle passing through a convergent orogen modeled on the Southern Alps, after Batt (1997) and Batt and Braun (1997, 1999). Convergence is at 10 mm/year, horizontal and vertical scales are equal, and the thermal structure shown is that developed after 5 Ma of deformation. The crosshatched region marks the peak strain rates in the model after 5 Ma and is interpreted to equate with the Alpine Fault for the Southern Alps (Fig. 5B). The white arrows show the exhumation trajectory of a selected particle. Also shown are the location at which the indicated particle begins to be exhumed and the site at which it undergoes closure for the zircon fission track chronometer, as discussed in the text. (C) Exhumation rates across the central Southern Alps as calculated from the zircon fission track ages by Tippett and Kamp (1993). Rates are plotted relative to the Alpine Fault, with the same horizontal scale as in panel B, to allow direct comparison between the two panels.

For example, Tippett and Kamp (1993) examined variation in orogenic kinematics for the Southern Alps by comparing the exhumation rates calculated from (1) the zircon fission track age data set and (2) estimates of the timing of initiation and total amount of exhumation across the orogen. Due to the convergence across the Southern Alps, these two parameters are in fact not directly comparable (Fig. 6). Each is the average exhumation rate over a finite duration (Fig. 1)—but the two are based on different time scales (one, the time since zircon fission track closure, the other, the time since the area in question first began to experience exhumation and cooling). With the marked variation in η calculated from Eq. (3) for these time scales ($\eta = 0.36$ for an average zircon fission track age of ca. 1 Ma and ca. 2.44 for the estimated ‘initiation of uplift’ in the Mt. Cook region at 6.7 ± 0.6 Ma, for example), lateral orogenic variation (Fig. 6) is integrated over correspondingly different length scales. These rate estimates would thus be expected to show relative differences, even had the Southern Alps remained at a kinematic steady state over the intervals concerned (Fig. 6B), and they are accordingly unable to provide a test of orogenic evolution over time.

By combining their fission track data with the K–Ar ages of Adams (1981), Tippett and Kamp (1993) also constructed a cooling curve for material adjacent to the Alpine Fault in the central Southern Alps (Fig. 6A). Variation in the observed cooling rate is interpreted to indicate varying kinematics for the Southern Alps as a whole and is the main support for their contention of a significant acceleration of orogenic activity over the past 1.3 ± 0.3 Ma (Tippett and Kamp, 1993). This interpretation departs markedly from the orogenic timing indicated by subsequent sedimentary (Sutherland, 1996) and regional tectonic (Sutherland, 1995; Walcott, 1998) studies, which indicate initial development of the modern orogenic dynamics of the Southern Alps at 5–6 Ma and little variation since that time.

This apparent disparity is resolved by the extent of lateral motion through the Southern Alps. A total of 90 ± 20 km of convergence have been accommodated across the Australian–Pacific plate boundary through the South Island over the past ca. 5 Ma (Walcott, 1998). The geology and structure of the orogen, however, indicate that it results from the deformation and exhumation of only the upper 20–25 km of the

Pacific plate crust (Fig. 5) (Wellman, 1979; Tippett and Kamp, 1993; Koons and Henderson, 1995; Beaumont et al., 1996; Walcott, 1998). Deeper crustal and mantle material detaches along a ductile décollement at depth (e.g. Wellman, 1979) and is either ductilely deformed into an orogenic root (Molnar et al., 1999) or ‘subducted’ together with the underlying lithospheric mantle as a coherent slab of material (e.g. Beaumont et al., 1996). Little, if any, of the material in the modern Southern Alps has thus been present in the orogen from its onset—and what remnants there are must have been translated significantly westwards relative to the plate boundary, with accompanying variation in the local orogenic conditions experienced over time (e.g. Wellman, 1979; Tippett and Kamp, 1993). Cooling histories of samples exposed in the orogen today will thus generally reflect the cycling of material through the established thermal structure of the Southern Alps, rather than the initiation and evolution of the orogen itself (Fig. 6).

Batt and Braun (1997, 1999) examined this issue through the numerical modeling of a Southern Alps-style orogen in two-dimensions. Early in the orogen’s development, the rapid exhumation perturbs the regional thermal structure, with isotherms dragged upwards by rapid advection of material, increasing the near-surface geothermal gradient, and producing a commensurate decrease in the thermal gradient at depth (Fig. 6B). Material subsequently entering this established system and approaching the plate boundary experiences a highly nonlinear increase in cooling rate leading up to its exposure at the surface. This takes the form of an initial period of slow cooling as this material passes through the reduced geothermal gradient at depth, followed by very rapid cooling as it is exhumed through the near surface thermal boundary layer (Fig. 6A). In the rapidly converging tectonic regime of the Southern Alps, even the profound variation in cooling rate documented by Tippett and Kamp (1993) is effectively ambiguous in its tectonic implications and requires no acceleration in the orogenic kinematics over time.

5. Conclusions

The physical implications of thermochronological data are ambiguous in regions subject to significant

lateral convergence between crustal blocks. Apparently discrete episodes of cooling or variation in rates of cooling under such conditions can be caused equally well by change in regional dynamics or by movement of material relative to the reference frame of the laterally inhomogeneous physical or thermal regime of the deforming region. This ambiguity confounds attempts to interpret thermochronology purely in terms of 1-D behavior and requires more computationally involved consideration and treatment.

Thermochronological ages at the surface of eroded regions generally reflect an integration of denudational and thermal conditions experienced between the isotopic closure of a sample and its subsequent exposure. When subject to lateral motion through the denuding region, different thermochronometers thus constrain not just different time scales but also different length scales of regional character, depending on their relative closure temperature. The higher the temperature at which a system closes, the deeper in the crust and the earlier closure occurs, the greater the lateral distance that will subsequently be traveled prior to exposure and the wider the potential range of lateral variation which will be incorporated into the observed age. The higher the closure temperature of a chronometer, the more sensitive it becomes to long-term behavior, the lateral path of the sample and regional variation in orogenic character. Conversely, the lower the temperature of a chronometer's closure, the less sensitive it is to lateral variation in orogenic character, and the more sensitive it is to local denudation conditions, surface processes, and topographic effects. Different chronometers constrain not just varying time scales or levels of sensitivity but provide insight into fundamentally different aspects of the character and evolution of convergent orogens.

Although lateral motion within a deforming region is difficult to directly constrain, such effects can be assessed qualitatively through numerical modeling. Numerical simulations coupling kinematic scenarios to thermal evolution allow interpretation of thermochronological data in a context consistent with their actual tectonic setting. This enables thermochronology to be used as an indication of the state of an evolving orogen through time, as long as its basic mode of deformation can be determined. As shown through case studies of the Olympic Mountains and the Southern Alps, such constraint offers useful

insight into the development of convergent orogens and can lead to the production of models more consistent with independent constraints on the tectonic history of such regions.

Acknowledgements

This work was produced while GEB was supported by a Damon Wells Post-doctoral Fellowship at Yale University. We thank the American Chemical Society Petroleum Research Fund for the partial support of this research. The authors are grateful for the opportunity to discuss and develop the ideas presented here in the intellectually fertile and congenial atmosphere of the FT2000 conference in Lorne. Insightful reviews and suggestions by Peter Zeitler and Mike Sandiford led to significant improvements in the communication of these concepts and are gratefully appreciated.

References

- Adams, J., 1980. Contemporary uplift and erosion of the Southern Alps, New Zealand. *Geological Society of America Bulletin*, vol. 91, pp. (I) 2–4, (II) 1–114.
- Adams, C.J., 1981. Uplift rates and thermal structure in the Alpine Fault zone and Alpine Schist, Southern Alps, New Zealand. In: McClay, K.R., Price, N.J. (Eds.), *Thrust and Nappe Tectonics*. Special Publication 9, Geological Society of London, London, pp. 211–222.
- Adams, C.J., Gabites, J.E., 1985. Age of metamorphism and uplift in the Alpine Schist Group at Haast Pass, Lake Wanaka and Lake Hawea, South Island, New Zealand. *New Zealand Journal of Geology and Geophysics* 28, 85–96.
- Allis, R.G., Shi, Y., 1995. New insights to temperature and pressure beneath the central Southern Alps, New Zealand. *New Zealand Journal of Geology and Geophysics* 38, 585–592.
- Batt, G.E., 1997. The Crustal Dynamics and Tectonic Evolution of the Southern Alps, New Zealand. Insights from new geochronological data and fully coupled thermo-dynamical finite element modeling. PhD thesis, Australian National University, Canberra, 273 pp.
- Batt, G.E., Braun, J., 1997. On the thermo-mechanical evolution of compressional orogens. *Geophysical Journal International* 128, 364–382.
- Batt, G.E., Braun, J., 1999. The tectonic evolution of the Southern Alps, New Zealand: insights from fully thermally coupled dynamical modeling. *Geophysical Journal International* 136, 403–420.
- Batt, G.E., Kohn, B.P., Braun, J., McDougall, I., Ireland, T.R., 1999. New insight into the dynamic development of the Southern Alps, New Zealand, from detailed thermochronological inves-

- tigation of the Mataketake Range pegmatites. In: Ring, U., Brandon, M., Lister, G., Willett, S. (Eds.), Special Volume on Exhumation Processes: Normal Faulting, Ductile Flow, and Erosion. Special Publication 154, Geological Society of London, London, pp. 261–282.
- Batt, G.E., Braun, J., Kohn, B.P., McDougall, I., 2000. Thermochronological analysis of the dynamics of the Southern Alps, New Zealand. *Geological Society of America Bulletin* 112, 250–266.
- Batt, G.E., Brandon, M.T., Farley, K.A., Roden-Tice, M., 2001. Tectonic synthesis of the Olympic Mountains segment of the Cascadia wedge, using 2-D thermal and kinematic modeling of isotopic age. *Journal of Geophysical Research* 106, 26731–26746.
- Beaumont, C., Fullsack, P., Hamilton, J., 1992. Erosional control of active compressional orogens. In: McClay, K.R. (Ed.), *Thrust Tectonics*. Chapman & Hall, New York, pp. 1–18.
- Beaumont, C., Kamp, P.J.J., Hamilton, J., Fullsack, P., 1996. The continental collision zone, South Island, New Zealand: comparison of geodynamical models and observations. *Journal of Geophysical Research* 101, 3333–3359.
- Beck Jr., M.E. 1991. Case for northward transport of Baja and coastal Southern California: paleomagnetic data, analysis, and alternatives. *Geology* 19, 506–509.
- Brandon, M.T., Calderwood, A.R., 1990. High-pressure metamorphism and uplift of the Olympic subduction complex. *Geology* 18, 1252–1255.
- Brandon, M.T., Vance, J.A., 1992. Tectonic evolution of the Cenozoic Olympic subduction complex, Washington State, as deduced from fission track ages for detrital zircon. *American Journal of Science* 292, 565–636.
- Brandon, M.T., Roden-Tice, M.K., Garver, J.I., 1998. Late Cenozoic exhumation of the Cascadia wedge in the Olympic Mountains, northwest Washington state. *Geological Society of America Bulletin* 110, 985–1009.
- Chamberlain, C.P., Poage, M.A., Craw, D., Reynolds, R.C., 1999. Topographic development of the Southern Alps recorded by the isotopic composition of authigenic clay minerals, South Island, New Zealand. *Chemical Geology* 155, 279–284.
- Clark, S.P., Jäger, E., 1969. Denudation rates in the Alps from geochronologic and heat flow data. *American Journal of Science* 267, 1143–1160.
- Clowes, R.M., Brandon, M.T., Green, A.G., Yorath, C.J., Sutherland Brown, A., Kanasewich, E.R., Spencer, C., 1987. LITHOPROBE—southern Vancouver Island: Cenozoic subduction complex imaged by deep seismic reflections. *Canadian Journal of Earth Sciences* 24, 31–51.
- Copeland, P., Harrison, T.M., Kidd, W.S.F., Ronghua, X., Yuquan, Z., 1987. Rapid early Miocene acceleration of uplift in the Gangdese Belt, Xizang (southern Tibet), and its bearing on accommodation mechanisms of the India–Asia collision. *Earth and Planetary Science Letters* 86, 240–252.
- Cutten, H.N.C., 1979. Rappahannock group: Late Cenozoic sedimentation and tectonics contemporaneous with Alpine Fault movement. *New Zealand Journal of Geology and Geophysics* 22, 535–553.
- Davey, F.J., Henyey, T., Kleffman, S., Melhuish, A., Okaya, D., Stern, T.A., Woodward, D.J., 1995. Crustal reflections from the Alpine Fault Zone, South Island, New Zealand. *New Zealand Journal of Geology and Geophysics* 38, 601–604.
- Davis, E.E., Hyndman, R.D., 1989. Accretion and recent deformation of sediments along the northern Cascadia subduction zone. *Geological Society of America Bulletin* 101, 1465–1480.
- DeMets, C.G., Gordon, R.G., Argus, D.F., Stein, S., 1990. Current plate motions. *Geophysical Journal International* 101, 425–478.
- Dodson, M.H., 1973. Closure temperatures in cooling geochronological and petrological systems. *Contributions to Mineralogy and Petrology* 40, 259–274.
- Dodson, M.H., 1979. Theory of cooling ages. In: Jaeger, E., Hunziker, C.J. (Eds.), *Lectures in Isotope Geology*. Springer-Verlag, New York, pp. 194–202.
- England, P.C., Richardson, S.W., 1977. The influence of erosion upon the mineral facies of rocks from different metamorphic environments. *Journal of the Geological Society (London)* 134, 201–213.
- England, P.C., Thompson, A.B., 1984. Pressure-temperature-time paths of regional metamorphism I: Heat transfer during the evolution of thickened continental crust. *Journal of Petrology* 25, 894–928.
- Fitzgerald, P.G., Gleadow, A.J.W., 1988. Fission-track geochronology, tectonics and structure of the Transantarctic Mountains in northern Victoria Land, Antarctica. *Chemical Geology* 73, 169–198.
- Garver, J.I., Brandon, M.T., 1994. Erosional denudation of the British Columbia Coast Ranges as determined from fission-track ages of detrital zircon from the Tofino Basin, Olympic Peninsula, Washington. *Geological Society of America Bulletin* 106, 1398–1412.
- Gleadow, A.J.W., Duddy, I.R., 1981. A natural long-term track annealing experiment for apatite. *Nuclear Tracks* 5, 169–174.
- Grapes, R.H., Watanabe, T., 1992. Metamorphism and uplift of the Alpine Schist in the Franz Josef-Fox Glacier area of the Southern Alps, New Zealand. *Journal of Metamorphic Petrology* 10, 171–180.
- Harrison, T.M., Copeland, P., Kidd, W.S.F., Lovera, O.M., 1995. Activation of the Nyainqntanglha Shear Zone: implications for uplift of the southern Tibetan Plateau. *Tectonics* 14, 658–676.
- Harrison, T.M., Leloup, P.H., Ryerson, F.J., Tapponnier, P., Lacassin, R., Chen, W., 1996. Diachronous initiation of transtension along the Ailao Shan–Red River shear zone, Yunnan and Vietnam. In: Yin, A., Harrison, T.M. (Eds.), *The Tectonic Evolution of Asia*. Cambridge Univ. Press, Cambridge, pp. 205–226.
- Harrison, T.M., Grove, M., Lovera, O.M., Catlos, E.J., 1998. A model for the origin of Himalayan anatexis and inverted metamorphism. *Journal of Geophysical Research* 103, 27017–27032.
- Hurley, P.M., Hughes, H., Pinson Jr., W.H., Fairbairn, H.W. 1962. Radiogenic argon and strontium diffusion parameters in biotite at low temperatures obtained from Alpine Fault uplift in New Zealand. *Geochimica et Cosmochimica Acta* 26, 67–80.
- Hyndman, R.D., Wang, K., 1993. Thermal constraints on the zone of major thrust earthquake failure: the Cascadia subduction zone. *Journal of Geophysical Research* 98, 2039–2060.
- Jamieson, R.A., Beaumont, C., Fullsack, P., Hamilton, J., 1996. Tectonic assembly of inverted metamorphic sequences. *Geology* 24, 839–842.

- Kamp, P.J.J., 1997. Paleogeothermal gradient and deformation style, Pacific front of the Southern Alps Orogen: constraints from fission track thermochronology. *Tectonophysics* 274, 37–58.
- Kamp, P.J.J., Tippett, J.M., 1993. Dynamics of Pacific plate crust in the South Island (New Zealand) zone of oblique continent–continent convergence. *Journal of Geophysical Research* 98, 16105–16118.
- Kamp, P.J.J., Green, P.F., White, S.H., 1989. Fission track analysis reveals character of collisional tectonics in New Zealand. *Tectonics* 8, 169–195.
- Koons, P.O., 1987. Thermal and mechanical consequences of rapid uplift in continental collision: an example from the Southern Alps. *Earth and Planetary Science Letters* 86, 307–319.
- Koons, P.O., 1994. Three-dimensional critical wedges: tectonics and topography in oblique collisional orogens. *Journal of Geophysical Research* 99, 12301–12315.
- Koons, P.O., Henderson, C.M., 1995. Geodetic analysis of model oblique collision and comparison to the Southern Alps of New Zealand. *New Zealand Journal of Geology and Geophysics* 38, 545–552.
- Laslett, G.M., Green, P.F., Duddy, I.R., Gleadow, A.J.W., 1987. Thermal annealing of fission tracks in apatite. *Chemical Geology* 65, 1–13.
- Lewis, T.J., Bentowski, W.H., Davis, E.E., Hyndman, R.D., Souther, J.G., Wright, J.A., 1988. Subduction of the Juan de Fuca plate: thermal consequences. *Journal of Geophysical Research* 93, 15207–15225.
- Mancktelow, N.S., Grasemann, B., 1997. Time-dependent effects of heat advection and topography on cooling histories during erosion. *Tectonophysics* 270, 167–195.
- McCaffrey, R., 1996. Estimates of modern arc-parallel strain rates in fore arcs. *Geology* 24, 27–30.
- McCaffrey, R., Goldfinger, C., 1995. Forearc deformation and great subduction earthquakes: implications for Cascadia offshore earthquake potential. *Science* 267, 856–859.
- McCrory, P.A., 1996. Tectonic model explaining divergent contraction directions along the Cascadia subduction margin, Washington. *Geology* 24, 929–932.
- Molnar, P., Anderson, H.J., Audoin, E., Eberhart-Phillips, D., Gledhill, K.R., Klosko, E.R., McEvilly, T.V., Okaya, D., Savage, M.K., Stern, T., Wu, F.T., 1999. Continuous deformation versus faulting through the continental lithosphere of New Zealand. *Science* 286, 516–519.
- Naeser, C.W., 1979. Thermal history of sedimentary basins: fission track dating of subsurface rocks. In: Scholle, P.A., Schlüger, P.R. (Eds.), *Aspects of Diagenesis*. Society of Economic Paleontologists and Mineralogists, Special Publication 26, Springer-Verlag, Berlin, pp. 109–112.
- Naeser, N.D., Naeser, C.W., McCulloh, T.H., 1989. The application of fission track dating to the depositional and thermal history of rocks in sedimentary basins. In: Naeser, N.D., McCulloh, T.H. (Eds.), *Thermal History of Sedimentary Basins*. Springer-Verlag, New York, pp. 157–180.
- Norris, R.J., Koons, P.O., Cooper, A.F., 1990. The obliquely convergent plate boundary in the South Island of New Zealand: implications for ancient collision zones. *Journal of Structural Geology* 12, 715–725.
- Oxburgh, E.R., Turcotte, D.L., 1974. Thermal gradients and regional metamorphism in overthrust terranes. *Eos, Transaction* 55, 442–443.
- Pazzaglia, F.J., Brandon, M.T., 2001. A fluvial record of long-term steady-state uplift and erosion across the Cascadia forearc high, western Washington State. *American Journal of Science* 301, 385–431.
- Pearson, C.F., Beavan, J., Darby, D.J., Blick, G.H., Walcott, R.I., 1995. Strain distribution across the Australian–Pacific plate boundary in the central South Island, from 1992 GPS and earlier terrestrial observations. *Journal of Geophysical Research* 100, 22071–22081.
- Quidelleur, X., Grove, M., Lovera, O.M., Harrison, T.M., Yin, A., Ryerson, F.J., 1997. Thermal evolution and strike slip history of the Renbu Zedong Thrust, southeastern Tibet. *Journal of Geophysical Research* 102, 2659–2679.
- Rau, W.W., 1973. Geology of the Washington coast between Point Grenville and the Hoh River: Washington Department of Natural Resources. *Geology and Earth Resources Division Bulletin* 66, 58 pp.
- Reyners, M., Cowan, H., 1993. The transition from subduction to continental collision: crustal structure in the North Canterbury region, New Zealand. *Geophysical Journal International* 115, 1124–1136.
- Ring, U., Brandon, M.T., Willett, S.D., Lister, G.S., 1999. Exhumation processes. In: Ring, U., Brandon, M.T., Lister, G.S., Willett, S.D. (Eds.), *Exhumation Processes: Normal Faulting, Ductile Flow and Erosion*. Special Publication 154. Geological Society of London, London, pp. 1–27.
- Ruppel, C., Hodges, K.V., 1994. Role of horizontal thermal conduction and finite time thrust emplacement in simulation of pressure–temperature–time paths. *Earth and Planetary Science Letters* 123, 49–60.
- Ruppel, C., Royden, L., Hodges, K.V., 1988. Thermal modeling of extensional tectonics: application to pressure–temperature–time histories of metamorphic rocks. *Tectonics* 7, 947–957.
- Shi, Y., Allis, R., Davey, F., 1996. Thermal modelling of the Southern Alps, New Zealand. *Pure and Applied Geophysics* 146, 469–501.
- Smith, E.G.C., Stern, T.A., O'Brien, B., 1995. A seismic velocity profile across the central South Island, New Zealand, from explosion data. *New Zealand Journal of Geology and Geophysics* 38, 565–570.
- Stern, T.A., 1995. Gravity anomalies and crustal loading at and adjacent to the Alpine Fault, New Zealand. *New Zealand Journal of Geology and Geophysics* 38, 593–600.
- Stewart, R.J., 1970. Petrology, metamorphism and structural relations of graywackes in the Western Olympic Peninsula, Washington. PhD Dissertation, Stanford University, Stanford, CA, 129 pp.
- Stüwe, K., White, L., Brown, R., 1994. The influence of eroding topography on steady-state isotherms. Applications to fission track analysis. *Earth and Planetary Science Letters* 124, 63–74.
- Sutherland, R., 1994. Displacement since the Pliocene along the southern section of the Alpine Fault, New Zealand. *Geology* 22, 327–330.
- Sutherland, R., 1995. The Australia–Pacific boundary and Ceno-

- zoic plate motions in the SW Pacific: some constraints from Geosat data. *Tectonics* 14, 819–831.
- Sutherland, R., 1996. Transpressional development of the Australia–Pacific boundary through southern South Island, New Zealand: constraints from Miocene–Pliocene sediments, Waiho-1 borehole, South Westland. *New Zealand Journal of Geology and Geophysics* 39, 251–264.
- Tabor, R.W., 1972. Age of the Olympic Metamorphism, Washington: K–Ar dating of low-grade metamorphic rocks. *Geological Society of America Bulletin* 83, 1805–1816.
- Tabor, R.W., Cady, W.H., 1978a. Geologic Map of the Olympic Peninsula: United States Geological Survey Map I-994, scale 1:250,000.
- Tabor, R.W., Cady, W.H., 1978b. The structure of the Olympic Mountains, Washington—analysis of a subduction zone. U.S. Geological Survey Professional Paper 1033, 38 pp.
- Tippett, J.M., Kamp, P.J.J., 1993. Fission track analysis of the late Cenozoic vertical kinematics of continental Pacific Crust, South Island, New Zealand. *Journal of Geophysical Research* 98, 16119–16148.
- Tippett, J.M., Kamp, P.J.J., 1995. Geomorphic evolution of the Southern Alps, New Zealand. *Earth Surface Processes and Landforms* 20, 177–192.
- Wagner, G.A., Reimer, G.M., 1972. Fission-track tectonics: the tectonic interpretation of fission track ages. *Earth and Planetary Science Letters* 14, 263–268.
- Wagner, G.A., Reimer, G.M., Jäger, E., 1977. Cooling ages derived by apatite fission-track, mica Rb–Sr and K–Ar dating: the uplift and cooling history of the Central Alps. *Memoir of the Institute of Geology and Mineralogy, University of Padova*, vol. 30. Istituto di Geologia e Mineralogia, Padua, pp. 1–27.
- Walcott, R.I., 1998. Modes of oblique compression: Late Cenozoic Tectonics of the South Island of New Zealand. *Reviews of Geophysics* 36, 1–26.
- Wang, K., 1996. Simplified analysis of horizontal stresses in a buttressed forearc sliver at an oblique subduction zone. *Geophysical Research Letters* 23, 2021–2024.
- Wellman, H.W., 1979. An uplift map for the South Island of New Zealand, and a model for uplift of the Southern Alps. In: Walcott, R.I., Cresswell, M.M. (Eds.), *The Origin of the Southern Alps*. Royal Society of New Zealand, Bulletin, vol. 18. The Royal Society of New Zealand, Wellington, pp. 13–20.
- Zeitler, P.K., Johnson, N.M., Naeser, C.W., Tahirkheli, R.A.K., 1982. Fission-track evidence for Quaternary uplift of the Nanga Parbat region, Pakistan. *Nature* 298, 255–257.